Available online at www.sciencedirect.com

ScienceDirect

Mendeleev Commun., 2018, **28**, 257–260

Mendeleev Communications

Electrochemical reduction, radical anions and solvation energies of 1,2,3,4-tetrafluoro-9,10-anthraquinone and its *N*-piperidyl derivatives in DMF and DMF–water mixtures

Leonid A. Shundrin,*[a,b] Irina G. Irtegova,*[a] Nadezhda V. Vasilieva[a] and Vladimir A. Loskutov[a]

[a] *N. N. Vorozhtsov Novosibirsk Institute of Organic Chemistry, Siberian Branch of the Russian Academy of Sciences, 630090 Novosibirsk, Russian Federation. Fax: +7 383 330 9752; e-mail: shundrin@nioch.nsc.ru, irteg@nioch.nsc.ru*

[b] *Department of Natural Sciences, Novosibirsk State University, 630090 Novosibirsk, Russian Federation*

DOI: 10.1016/j.mencom.2018.05.009

The electrochemical reduction of 1,2,3,4-tetrafluoro-9,10-anthraquinone and its 2-(*N*-piperidyl) derivative in DMF and DMF–H_2O mixtures represents an EE-process, whereas that for 1-(*N*-piperidyl) and 1,4-di(*N*-piperidyl) derivatives occurs as an EEC-process. Based on the linear dependences of the first reversible one-electron reductive half-wave potentials of these compounds on the water content of DMF–H_2O mixtures, the corresponding changes in the free energies of solvation under electron transfer have been calculated. Radical anions of the above compounds were obtained in DMF and characterized by EPR spectroscopy and DFT calculations at the (U)B3LYP/6-31+G* level of theory.

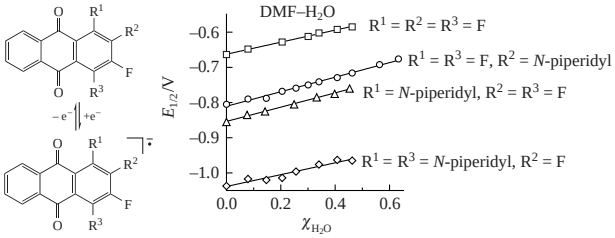

Anthraquinone (AQ) and its derivatives possess biological activity,[1–3] and they are used for cancer therapy in medicine[4,5] and also as redox active labels in DNA biosensor technologies,[6,7] receptors for selective fluoride ion recognition,[8] for the synthesis of dyes[9] and as pendant groups of electro-active polymers used in non-volatile memory devices.[10] Their applications are determined by reversible electron transfer in organic solvents and water media.[11,12] The replacement of hydrogen atoms with fluorine atoms in anthraquinone cycle leads to an increase in electron accepting ability, and it is accompanied by a shift of electrochemical reductive potentials towards less negative values.[13] A key property of the fluorinated AQs is a high reactivity of fluorine atoms towards nucleophilic substitution.[14] Based on this, fluorinated AQ derivatives have been synthesized and solvent and temperature effects were studied.[15–17] On the other hand, the high reactivity of fluorinated AQs can be used to bind the fluorinated AQs to electrochemically inactive molecules containing nucleophilic groups. From this point of view, fluorinated AQs are promising redox active labels because their electrochemical reduction potentials differ from the potentials of their H-containing congeners and other quinones used in electrochemical biosensor technologies.[18,19]

Despite the fact that fluorinated AQs are well known, only the electrochemical reduction (ECR) of 1,2,3,4-tetrafluorinated AQ **1** in CH_2Cl_2 has been studied.[13] The electrochemistry of fluorinated AQs with *N*-cycloalkyl substituents has not been investigated. In this work, we studied the ECR of fluorinated *N*-piperidyl-9,10-anthraquinones, which are the products of the reaction between **1** and an N-nucleophile. The synthesis of compounds **2**–**4** was described elsewere.[15]

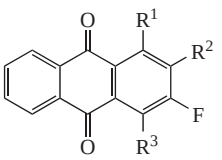

1 $R^1 = R^2 = R^3 = F$
2 R^1 = *N*-piperidyl, $R^2 = R^3 = F$
3 $R^1 = R^3 = F$, R^2 = *N*-piperidyl
4 $R^1 = R^3$ = *N*-piperidyl, $R^2 = F$

Cyclic voltammograms (CVs)† of **1**–**4** in DMF demonstrate different types of ECR behavior for **1**, **3** [Figure 1(*a*),(*c*)] and compounds **2**, **4** bearing substituents at the 1,4-positions of the fluoroanthraquinone ring [Figure 1(*b*),(*d*)]. The ECR of compounds **1**, **3** is an EE-process with two reversible one-electron peaks corresponding to the formation of a radical anion (RA) and a dianion (DA), which is a typical behavior of AQs in aprotic solvents. The first reduction peaks in CVs of **2**, **4** are reversible and diffusion controlled in DMF [Figure 1(*b*),(*d*) and Figure S1, see Online Supplementary Materials] indicating the long-lived nature of corresponding RAs, whereas the transfer of a second electron onto RAs **2**, **4** leads to the instability of DAs **2**, **4** and the irreversibility of peaks 2C in both cases [Figure 1(*b*),(*d*)].

† The CV measurements of AQs **1**–**4** in DMF and its mixtures with H_2O (1.2–1.7 mM solutions) were performed at 295 K under argon atmosphere. The supporting electrolyte was 0.1 M Et_4NClO_4. A PG 310 USB potentiostat (HEKA Elektronik) was used for the measurements. A standard electrochemical cell with a solution volume of 5 ml connected to the potentiostat with a three-electrode scheme was employed. A stationary Pt disk electrode (S = 0.06 cm^2) was used as a working electrode, and Pt helix was an auxiliary electrode. Peak potentials were quoted with reference to a saturated calomel electrode (SCE). A salt bridge with 0.1 M of supporting electrolyte in DMF and its mixtures with H_2O of the same composition as in working electrode space was used to connect the cell and SCE. Triangular potential sweep was used for CV measurements. The potential sweep rates were ν = 0.1–1.5 V s^{-1}. To estimate the pure resistance (R) of a cell and its changes when DMF–H_2O mixtures were used as a solvent, the corresponding measurements have been done using an INSTEK LCR meter. The signal frequency was 2 kHz.

Table 1 Peak potentials,[a] DFT calculated first adiabatic gas-phase electron affinities[b] (EA_1), and corresponding changes in the free energies of solvation ($\delta\Delta G^0_{solv}$) under one-electron transfer of **1**–**5** in DMF.

Compound	E_p^{iC}/V		E_p^{iA}/V			$E^1_{1/2}$/V	EA_1/eV	EA_{ad}/kcal mol^{-1}	$-\delta\Delta G^0_{solv}$/kcal mol^{-1}
	i = 1	i = 2	i = 1	i = 2	i = 3				
1	–0.698	–1.382	–0.626	–1.308	–	–0.662	1.567	45.41[c]	47.89
2	–0.887	–1.403	–0.818	–1.326	–0.56	–0.853	1.374	40.97[c]	47.92
3	–0.840	–1.474	–0.770	–1.404	–	–0.805	1.421	42.05[c]	47.99
4	–1.068	–1.610	–1.007	–	–0.74	–1.037	1.256	38.25[c]	46.44
5	–0.890	–1.540	–0.800	–1.460	–	–0.845	1.185	36.61[d]	54.40[e]

[a] Measured with Pt working electrode *vs.* SCE, v = 0.1 V s^{-1}; in potentials designation, $E_p^{iC(A)}$, i is a number of peak, symbols 'A' or 'C' indicate the anode or cathode branch of the CV curve. [b] EA_1 calculated at the B3LYP level of theory. [c] Recalculated values, $EA_{ad} = EA_1 + \Delta EA$, $\Delta EA = EA_{ad}$(**5**) – EA_1(**5**), EA_{ad}(**5**) is the experimental first gas-phase electron affinity of unsubstituted 9,10-anthraquinone (see ref. 20). [d] Experimental value in the following approximation: EA_{ad}(**5**) ≈ $-H_{ad}$(**5**) (see ref. 21). [e] Calculated with experimental EA_{ad}(**5**) (see ref. 21).

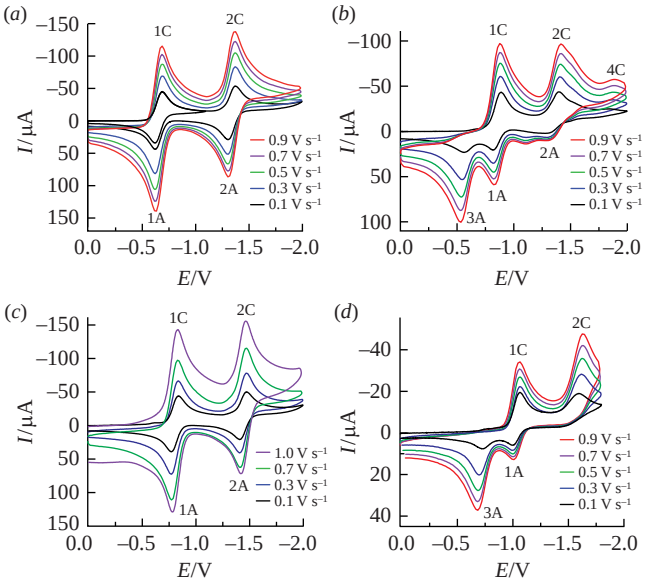

Figure 1 CVs of (*a*) **1**, (*b*) **2**, (*c*) **3**, (*d*) **4** in DMF in the potential sweep range 0 > E > –2.0 V at various potential sweep rates.

The peak 2C becomes quasi-reversible for **2** at the potential sweep rates v > 0.3 V s^{-1} [Figure 1(*b*)] and the corresponding anodic peak 2A becomes observable. No quasi-reversibility of 2C peak was detected for **4** in the studied range of v [Figure 1(*d*)].

Anodic peaks 3A were observed in the CVs of **2** and **4**, if the potential sweep range covers both peaks 1C, 2C only (Figure S2, see Online Supplementary Materials). This fact indicates the attribution of peaks 3A to electrochemical oxidation of unknown products of DAs transformation. An additional minor peak 4C was detected for the ECR of **2** [Figure 1(*b*)], whose nature was not studied.

Tentatively, the instability of DAs **2**, **4** can be explained by the higher reactivity of fluorine atoms at the 2,3-positions than that at the 1,4-positions, as was also observed in the nucleophilic substitution reactions of **1**.[15–17] The presence of electron donating substituents at the 1,4-positions of the AQs cycle activates the reactivity of fluorine atoms at the 2,3-positions and DAs **2**, **4** become less stable. The substitution in the 2-position does not activate the reactivity of fluorine atoms since no instability of DA **3** was observed [Figure 1(*c*)]. The electrochemical decomposition details of DAs **2**, **4** require a separate investigation.

Peak potentials of **1**–**4** together with the corresponding values $E^1_{1/2} = (E_p^{1C} + E_p^{1A})/2$‡ for the first reversible peaks and DFT calculated first adiabatic electron affinities are given in Table 1. Peak potentials of unsubstituted AQ **5** are presented for comparison.

For AQs **1**–**4**, a good correlation was revealed between the half-wave potentials of the first CV wave, $E^1_{1/2}$, and EA_1 values calculated by DFT [Figure 2(*a*)] indicating a uniform change of electron affinity in **1**–**4** in accordance with the electron donating effects of substituents. To estimate changes in the free energies of solvation ($\delta\Delta G^0_{solv}$) in **1**–**4**, it is necessary to correct the DFT calculated EA_1 values using the known experimental gas-phase electron affinity of a related compound as a reference point. The values of $\delta\Delta G^0_{solv}$ together with gas-phase electron affinities determine the first peak potentials and $E^1_{1/2}$ of **1**–**4** in solution, and they are related to charge distributions in their RAs.[20] Among the test compounds, the experimental gas-phase electron affinity EA_{ad} of 1.59 eV (36.61 kcal mol^{-1}, see Table 1) is known only for **5**, as found from electron transfer equilibria.[21] The difference in the DFT calculated and the experimental EA_{ad} of **5** is ΔEA = = 0.405 eV (9.326 kcal mol^{-1}), which was used to correct the DFT calculated EA_1 of **1**–**4** to obtain the corresponding EA_{ad} (see Table 1). Assuming the approximation $EA_{ad} \approx -\Delta H_{ad} \approx -\Delta G_{ad}$ due to minimal changes in entropy under electron transfer, it is easy to obtain a relationship between $E^1_{1/2}$, gas-phase electron affinity and $\delta\Delta G^0_{solv}$ as follows:[21,22]

$$\delta\Delta G^0_{solv} = -23.06E^1_{1/2} - \Delta G^0_{ad} + C, \quad (1)$$

where C = –108.6 kcal mol^{-1}, which includes the potential of SCE. This value of C was confirmed by published data.[23] Using the experimental EA_{ad} and $\delta\Delta G^0_{solv}$ of **5** in DMF as a reference point[21] the corresponding changes in free energies of solvation in DMF were calculated from equation (1) (see Table 1).

ECR of **1**–**4** in DMF–H_2O mixtures in the range of the molar fractions of water 0 < χ < 0.6 led to consequent shifts of both E_p^{iC} (i = 1,2) and the corresponding $E^1_{1/2}$ potentials towards less negative values [Figure 2(*b*), Figure S3, Tables S1–S4]. The values of $E^1_{1/2}$ in H_2O obtained by extrapolation of $E^1_{1/2}(\chi = 1)$ are –0.491, –0.651, –0.604, and –0.870 V, respectively (*vs.* SCE). In the range 0 < χ < 0.46 the solvent dependences of $E^1_{1/2}$ associated with the first reductive one-electron CV wave of **1**–**4** form parallel linear regressions [Figure 2(*b*)] and allow us to estimate the corresponding dependences of $\delta\Delta G^0_{solv}$ on water contents (Tables S1–S4) using the same constant C [equation (1)]. The effect of diffusion potential changes on $E^1_{1/2}$ at various χ limits the range of χ for the correct determination of $\delta\Delta G^0_{solv}$ (χ) by 0 < χ < 0.46.

The linear dependences $\delta\Delta G^0_{solv}$ (χ) demonstrate an increase in the absolute values of $|\delta\Delta G^0_{solv}|$ with χ, as it was previously observed.[20] The difference in $\delta\Delta G^0_{solv}$ (χ) is noticeable only for compound **4** with two *N*-piperidyl substituents at the 1,4-positions of the AQ ring [Figure 2(*c*)]. Since the $\delta\Delta G^0_{solv}$ values are mostly determined by electrostatic interactions of RAs with solvent molecules,[20,22] it can be concluded that RA **4** is characterized by the least intense electrostatic interaction with solvent

‡ For discussion of *IR*-compensation effect on the $E^1_{1/2}$ and for a contribution of diffusion potential in $E^1_{1/2}$ values, see Online Supplementary Materials.

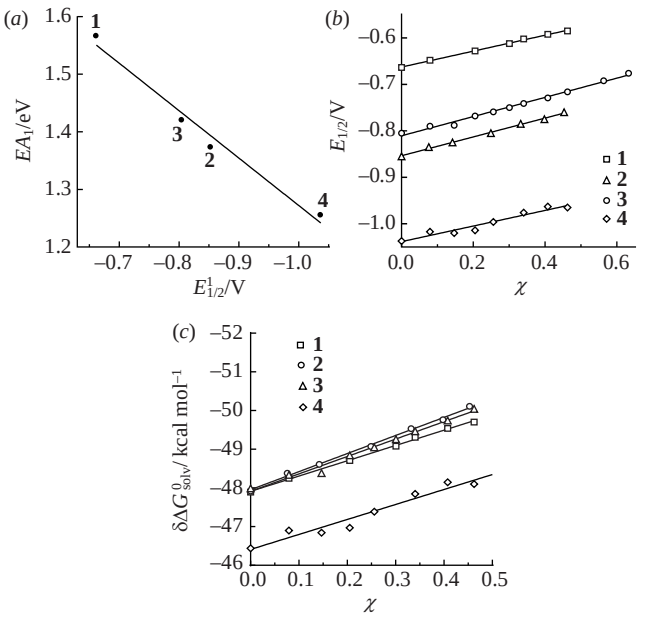

Figure 2 (*a*) Correlation between calculated gas-phase EA_1 and first reduction half-wave potentials $E^1_{1/2}$ of **1**–**4** in DMF, (*b*) solvent dependences of $E^1_{1/2}$ for the first electron transfer process onto **1**–**4** in DMF–H_2O mixtures, (*c*) the dependences of changes in free energy of solvation of **1**–**4** under electron transfer on water molar fraction in DMF–H_2O mixtures.

molecules among compounds **1**–**4**. Tentatively, it can be explained by a shielding effect from two *N*-piperidyl substituents in the 1,4-positions of **4**, which hinders interactions between RA **4** and solvent molecules. Note that the $\delta\Delta G^0_{solv}$ values of fluorinated AQs will be useful for computational studies of solvent effects on the reduction potentials of anthraquinone derivatives.[26]

For compounds **1**–**4**, the EPR spectra[§] of the RAs were obtained under stationary electrolysis in DMF at the potentials E^{iC}_p (Figure S4). The EPR spectrum of RA **1** (Table 2, Figure S4) demonstrated the pared magnetic equivalence of ^{19}F (1,4- and 2,3-positions) and ^1H (5,8- and 6,7-positions) nuclei and a well-resolved hyperfine structure (hfs) with all nuclei except for ^1H (5,8). For RAs **2**–**4**, hfs with ^{19}F and ^1H (6,7) is resolved and no hfs with ^{14}N and ^1H (5,8) nuclei were detected due to the low values of the corresponding hyperfine coupling (hfc) constants that are comparable with the line width. For RAs **1**–**4**, no hfs with ^1H nuclei of the *N*-piperidyl ring were observed.

The experimental isotropic hfc constants of the RAs together with those calculated in a gas phase at the (U)B3LYP/6-31+G* level of theory[¶] (see Table 2) demonstrate good compatibility. According to calculations, the fluoroanthraquinone scaffold is planar in all RAs, and SOMO is of π-type (Figure S5). The *N*-piperidine cycle in RAs **2**–**4** has a chair conformation twisted

Table 2 Experimental[a] and gas-phase DFT-calculated isotropic hfc constants (G) of RAs **1**–**4**.

RA	Experiment	(U)B3LYP/6-31+G*
1	0.27 ($F^{1,4}$), 3.56 ($F^{2,3}$), 0.05 ($H^{5,8}$), 0.71 ($H^{6,7}$)	–0.475 ($F^{1,4}$), 2.624 ($F^{2,3}$), –0.043 ($H^{5,8}$), –0.856 ($H^{6,7}$)
2[b]	0.19 (N), 2.99 (F^2), 4.34 (F^3), 0.95 (F^4), 0.71 (H^6), 0.37 (H^7)	0.096 (N), 1.810 (F^2), 2.893 (F^3), –0.898 (F^4), 0.055 (H^5), –0.982 (H^6), –0.770 (H^7), –0.139 (H^8)
3[c]	0.92 (F^1), 0.15 (N), 2.65 (F^3), 0.53 (H^6), 0.70 (H^7)	–1.435 (F^1), –0.259 (N), 2.693 (F^3), –0.129 (F^4), –0.170 (H^5), –0.665 (H^6), –0.970 (H^7), 0.099 (H^8)
4	0.17 ($N^{1,4}$), 4.46 ($F^{2,3}$), 0.37 ($H^{5,8}$), 0.87 ($H^{6,7}$)	0.022 (N^1), 2.000 (F^2), 2.045 (F^3), 0.047 (N^4), –0.038 (H^5), –0.877 (H^6), –0.863 (H^7), –0.052 (H^8)

[a] In DMF, numbers of RAs correspond to those of their neutral precursors; numbers of atoms H and F are the same as for C atoms they are bound with. [b] EPR spectrum has unresolved hfc constants with $H^{5,8}$. [c] EPR spectrum has unresolved hfc constants with F^4 and $H^{5,8}$.

from the AQ cycle plane (Figure S5, Tables S7–S10) and two *N*-piperidyl cycles in RA **4** are in a hindered conformation with respect to each other. Note that DFT calculations indicate a positive sign of the hfc constants with ^{19}F (2,3) nuclei, whereas hfc constants with other nuclei are negative (see Table 2).

In conclusion, we described the electrochemical behavior of *N*-piperidyl-substituted fluorinated anthraquinones in DMF and its mixtures with H_2O. ECR of **3** in DMF is analogous to that for 1,2,3,4-tetrafluoroanthraquinone **1** and is a classical EE process, whereas ECR of **2**, **4** is the EEC process and their dianions are unstable both in DMF and in its mixtures with water. For all AQs studied, linear dependences of the first CV half-wave potentials $E^1_{1/2}$ on water content in a range of $0 < \chi < 0.462$ were found to reflect changes in the free energy of solvation, and the weakest absolute values of $\delta\Delta G^0_{solv}$ were observed for compound **4**.

Finally, note that, taking into account the low values of the extrapolated ECR potentials of compounds **1**–**3** in H_2O and the high reactivity of fluorine atoms in nucleophilic substitution reactions,[15–17] we can suggest the practical application of the test fluorinated anthraquinones as redox active labels for the modification of oligonucleotides in biosensory technologies.[19]

This study was supported by the Russian Foundation for Basic Research (grant no. 17-03-00944-a). We are grateful to the Multi-Access Center Chemical Service, Siberian Branch of the Russian Academy of Sciences, for instrumental facilities.

Online Supplementary Materials

Supplementary data associated with this article can be found in the online version at doi: 10.1016/j.mencom.2018.05.009.

References

1 W. A. Cramer and D. B. Knaff, in *Energy Transduction in Biological Membranes*, ed. C. R. Cantor, Springer, New York, 1990, ch. 4, pp. 141–192.
2 R. A. Morton, *Biochemistry of Quinones*, Academic Press, New York, 1965.
3 H. Beraldo, A. Garnier-Suillerot, L. Tosi, and F. Lavelle, *Biochemistry*, 1985, **24**, 284.
4 V. J. Ferrans, *Cancer Treat. Rep.*, 1978, **62**, 955.
5 A. Ashnagar, J. M. Bruce, P. L. Dutton and R. C. Prince, *Biochim. Biophys. Acta*, 1984, **801**, 351.
6 S. Kumamoto, M. Watanabe, N. Kawakami, M. Nakamura and K. Yamana, *Bioconjugate Chem.*, 2008, **19**, 65.
7 Y. Liu and N. Hu, *Biosens. Bioelectron.*, 2007, **23**, 661.
8 A. A. Vavilova, R. V. Nosov and I. I. Stoikov, *Mendeleev Commun.*, 2016, **26**, 508.
9 P. F. Gordon and P. Gregory, *Organic Chemistry in Colour*, Springer, Berlin, Heidelberg, 1987.
10 H.-J. Yen, K.-Y. Lin and G.-S. Liou, *J. Polym. Sci., Part A: Polym. Chem.*, 2012, **50**, 61.

[§] The EPR spectra of RAs **1**–**4** were measured with an ELEXSYS E-540 spectrometer (X-band, MW frequency, ~9.87 GHz; MW power, 1 mW; modulation frequency, 100 kHz; and modulation amplitude, 0.006 mT) equipped with a high-Q cylindrical resonator ER4119HS. For the EPR measurements stationary ECR of compounds **1**–**4** at corresponding first peak potentials was carried out at 295 K under anaerobic conditions. Electrochemical cell for EPR measurements equipped with Pt working electrode was placed in the EPR cavity. Electrolysis was performed in dry DMF with 0.1 M Et_4NClO_4 as a supporting electrolyte. Simulations of the experimental EPR spectra were accomplished with the Winsim 2002 program.[24] The Simplex algorithm was used for optimization of hfc constants and line widths.

[¶] The DFT calculations on compounds **1**–**4** and their RAs were performed with full geometry optimization (Tables S7–S10, see Online Supplementary Materials) at the (U)B3LYP/6-31+G* level of theory using the GAMESS program.[25]

11 J. Q. Chambers, in *The Chemistry of Quinonoid Compounds*, eds. S. Patai and Z. Rappoport, Wiley, New York, 1988, vol. 2, ch. 12, pp. 719–757.
12 K. Sasaki, T. Kashimura, M. Ohura, Y. Ohsaki and N. Ohta, *J. Electrochem. Soc.*, 1990, **137**, 2437.
13 N. Martın, P. de Miguel, C. Seoane, A. Albert and F. H. Cano, *J. Mater. Chem.*, 1997, **7**, 25.
14 O. Bayer, *Meth. Org. Chem.* (*Houben–Weyl*), 1979, **7**(3c), 65.
15 V. A. Loskutov and E. P. Fokin, *Zh. Obshch. Khim*., 1968, **38**, 1884 (in Russian).
16 V. A. Loskutov, *Russ. J. Org. Chem.*, 2013, **49**, 1470 (*Zh. Org. Khim.*, 2013, **49**, 1492).
17 V. A. Loskutov, S. M. Lukonina, A. V. Konstantinova and E. P. Fokin, *Zh. Org. Khim.*, 1981, **17**, 584 (in Russian).
18 D. A. Di Giusto, W. A. Wlassoff, S. Giesebrecht, J. J. Gooding and G. C. King, *J. Am. Chem. Soc.*, 2004, **126**, 4120.
19 L. A. Shundrin, I. G. Irtegova, N. V. Vasilieva and I. A. Khalfina, *Tetrahedron Lett.*, 2016, **57**, 392.
20 G. W. Dillow and P. Kebarle, *Can. J. Chem.*, 1989, **67**, 1628.
21 T. Heinis, S. Chowdhurry, S. L. Scott and P. Kebarle, *J. Am. Chem. Soc.*, 1988, **110**, 400.
22 L. A. Shundrin, I. G. Irtegova, N. V. Vasilieva, P. A. Avrorov, N. Yu. Selikhova, A. G. Makarov, A. Yu. Makarov, Yu. G. Slizhov and A. V. Zibarev, *J. Phys. Org. Chem.*, 2017, **30**, e3667.
23 (*a*) J. T. Farrell and P. J. McTigue, *J. Electroanal. Chem.*, 1982, **139**, 37; (*b*) H. Reiss and A. Heller, *J. Phys. Chem.*, 1985, **89**, 4207.
24 R. D. Duling, *J. Magn. Reson.*, 1994, **104**, 105.
25 M. W. Schmidt, K. K. Baldridge, J. A. Boatz, S. T. Elbert, M. S. Gordon, J. H. Jensen, S. Koseki, N. Matsunaga, K. A. Nguyen, S. Su, T. L. Windus, M. Dupuis and J. A. Montgomery, Jr., *J. Comput. Chem.*, 1993, **14**, 1347.
26 D. Ajloo, B. Yoonesi and A. Soleymanpour, *Int. J. Electrochem. Sci.*, 2010, **5**, 459.

Received: 13th November 2017; Com. 17/5404